

Supplemental Information: Harnessing genetic variation in leaf angle to increase productivity of

Sorghum bicolor

Sandra K. Truong^{1,2}, Ryan F. McCormick^{1,2}, William L. Rooney³, and John E. Mullet^{1,2,*}

1 Interdisciplinary Program in Genetics, Texas A&M University, College Station, Texas 77843

2 Biochemistry & Biophysics Department, Texas A&M University, College Station, Texas 77843

3 Soil & Crop Sciences Department, Texas A&M University, College Station, Texas 77843

* Corresponding Author: John E. Mullet
300 Olsen Boulevard
College Station, TX 77843-2128
(979) 845 0722
jmullet@tamu.edu

File S1

Extended Materials and Methods

Calculation of the light extinction coefficient, k .

Light interception throughout crop canopies is often formalized as an extinction coefficient, k (as derived in Beer-Lambert's Law), that relates the attenuation of light with properties of the material through which the light travels (MONTEITH 1977; MONSI AND SAEKI 2005; NOBEL 2005; LONG *et al.* 2006). Here, we describe adoption of Beer-Lambert equations in the context of solar radiation attenuation through a sorghum canopy to characterize and compare the distribution of light in simulated and field grown sorghum canopies with differing leaf inclination angles.

Let $I(x)$ be the intensity, power per unit area, of radiation from the sunlight at depth x down the canopy. For any given time at a plane above the canopy, $x = 0$, the intensity of radiation from the sun is at its maximum as no radiation has been intercepted, $I(0) = \max_x I(x)$. A sequence of planes, parallel to the ground, moving from the top, $x = 0$, down to the ground level of the canopy will have decreasing amounts of transmitted radiation, as each plane in the canopy intercepts a portion of the radiation. As such, the rate of radiation or light extinction when moving down the canopy, $\frac{dI}{dx}$, can be represented as

$$\frac{dI}{dx} = -kI(x), \quad (1)$$

where k is a dimensionless variable that represents the proportion of radiation intercepted at depth x down the canopy. By integration of Equation 1 and the initial condition $I(0) = I_0$,

$$I(x) = I_0 e^{-kx} \quad (2)$$

Thus given data, $\{x_n, I(x_n)\}_{n=1}^N$, that can be reasonably described by Equation 2, we can find light extinction coefficient, k , and use this as a descriptor for the distribution of light down a sorghum canopy. We defined I_0 , the top of canopy, to be the plane immediately below the whorls of plants in the canopy. We distinguish between two groups of leaves in a sorghum canopy: (i) the whorl, the top of the plant from which leaves emerge, (ii) and leaves that are fully expanded below the whorl. The whorl contains leaves that are essentially in the same plane, whereas fully expanded leaves share less planes with other leaves above and below it. We found better fits to light data when fitting data just below the whorl to find the light extinction coefficient, k_2 , however the relative relationship between small and large leaf inclinations angles remained regardless of where we defined the top of the canopy. The next sections will describe the method used to collect the data in both simulated and field experiments to estimate light extinction coefficients, k s. Specifically, k values for simulated and experimental data were solved for by the Levenberg-Marquardt algorithm for non-linear least-squares as implemented in the open source software SciPy's `scipy.optimize.curve_fit()` function (JONES 2001).

Virtual sorghum canopies.

In order to calculate theoretical k s we constructed functional-structural plant models of sorghum and collected depth and incident light data, $\{x_n, I(x_n)\}_{n=1}^N$, in simulated light environments. The 3-dimensional virtual sorghum plants were constructed using Lindenmeyer systems in L-py (BOUDON *et al.* 2012). Lindenmeyer-systems provide a set of production rules whereby plant structural models are produced by recursion through phytomers (PRUSINKIEWICZ *et al.* 2012). As such, virtual sorghum was constructed from phytomers, characterized by a stem and a leaf that emerges on top of one other. Thus each sorghum plant has a set of phytomers $p = p_1, p_2, \dots, p_N$ where p_1 is the first phytomer to emerge and closest to the bottom and p_N is the last fully emerged phytomer at the top of the plant; only the colored phytomers are considered to calculate k_2 (Figure 2a). These virtual plants were then replicated to simulate sorghum plots that have typical row spacing of 0.76 m and planting density of 13.2 plants/m². Since the phytomers appear one on top of another and are uniformly distanced from the ground in the virtual environment, fully emerged phytomers, p_i , are used as depth measurements in the virtual sorghum canopies. When the simulated sorghum genotypes varied in the number of the phytomers (and consequently height) as they did when simulating plants with the characteristics of RIL 63 and RIL 73 of the R07018 x R07020 recombinant inbred line population, the height difference was accounted for by scaling depth to be a percentage depth, such that $x_n := 100 \frac{p_n}{p_N}$. The qualitative relationship of the rates of extinction between canopies with large and small leaf angles remains the same whether or not scaling is performed; scaling height just removes an unnecessary complexity.

The virtual canopies were then illuminated by the nested radiosity model as implemented in CARIBU (CHELLE AND ANDRIEU 1998; CHELLE 2004) given light input that reflected solar conditions in College Station, TX (data retrieved from The United States Naval Observatory). The illuminated sorghum canopies could then be visualized (see Supporting Information for a .gif time course of lighting over a day). The nested radiosity model enables the estimation of absorbed energy or irradiance of each phytomer. Construction and lighting of the virtual canopies were all done within the open source software OpenAlea v1.0 that integrates L-py and Caribu, among other functional-structural modeling tools (PRADAL *et al.* 2008). Let $Eabs(p_n)$ be the energy absorbed by phytomer n , p_n . Then to extract the amount of energy or incident light available, $I(x_n)$, at x_n

$$I(x_n) = \sum_{i=1}^N Eabs(p_i) - \sum_{i=n}^N Eabs(p_i).$$

With Equation 2 and p_n defined, this provides data, $\{x_n, I(x_n)\}_{n=1}^N$, to fit to Equation 2 in order to estimate ks for virtual sorghum canopies. Input files and scripts to reproduce virtual sorghum canopies used here are accessible on GitHub (see Supplemental Information).

Field experimental sorghum canopies.

To collect incident light data at different depths in the sorghum canopies, two lifts for PAR meters were used to take simultaneous readings in two plots of sorghum. Each of the two plots contained four rows of the same genotype, where the two genotypes varied in their leaf inclination angle. Two sorghum recombinant inbred lines, RIL 63 and RIL 73, were identified as RILs that had varying inclination angles under genetic regulation when QTL mapping was performed in a RIL population generated from a biparental cross of the energy sorghum lines R07018 and R07020 (BARTEK 2012). These two genotypes were then planted in 4 row plots with row spacing of 0.76 m^2 and planting density of 13.2 plants/m^2 in College Station, TX fields (W 96 20, N 30 37).

The consistent depths at which incident sunlight was captured in the canopies were ensured by using two pulley systems that were individually manned. Figure S3 shows the pulley and the PAR meters, LP-80 from Decagon Devices. The platforms holding the LP-80 were raised and lowered in increments of 1 ft (0.3048 m) that were marked on the pulley string to guide the depth in canopy where n are the depth measurements that the PAR meter is n ft from ground, $n = 1, \dots, 14$. The genotypes were different heights at the time of measurement, during their vegetative stage; percentages of depth with respect to height of genotype, $h_{genotype}$, in the canopies are used such that $x_n := 100 \frac{n}{h_{genotype}}$. The rates of extinction for large and small leaf angle canopies remained the same whether or not depth was scaled, so depth was scaled to remove complexity. One set of readings represents the depths measured from top to bottom or bottom to top by the operators. To mitigate operational biases, the operators, PAR meters, and pulley systems were often swapped between plots. Lastly, consistency of external light conditions between the plots were maintained by using the two PAR meters and coordination between the operators so that the same depths were assayed simultaneously in both plots. Two of the sets of data, those taken on July 25th, were taken after the plots had been thinned to a lesser density; the change in plot density increased the amount of PAR available at lower levels in the canopy, but did not change the relative trend of light extinction (Table S2).

The platform and pulley mechanism was designed to reduce interference with the 0.865 m probe that contains 80 PAR sensors and was used in between the two middle rows of the 4 row plots. The instrument was set to log PAR data, $I(t)$, automatically at 1 minute intervals, and 3 minutes were spent at each level in the canopy and recorded to ensure that at least two data points were captured at each level in the canopy. It took users manning the instruments different amounts of time to move the platform to the next level, and so data for the 3 minutes at each level began when both platforms were at the prescribed depth and cloud cover was absent. Light interception in the two plots was simultaneously assayed to ensure that the amount of available sunlight, I_0 , was similar. Light intercepted at a given depth was taken as the average of logged PAR measurements that were available in the 3 minute windows. Let the 3 minute interval at depth x_n be $(t_0, t_T)_n$, then $I(x_n) := \text{average}_{t \in (t_0, t_T)_n} I(t)$. All plot and plant measurements along with raw depth from the experimental field data and subsequent scaling employed and their fits to Equation 2 are available in the Supplemental Information.

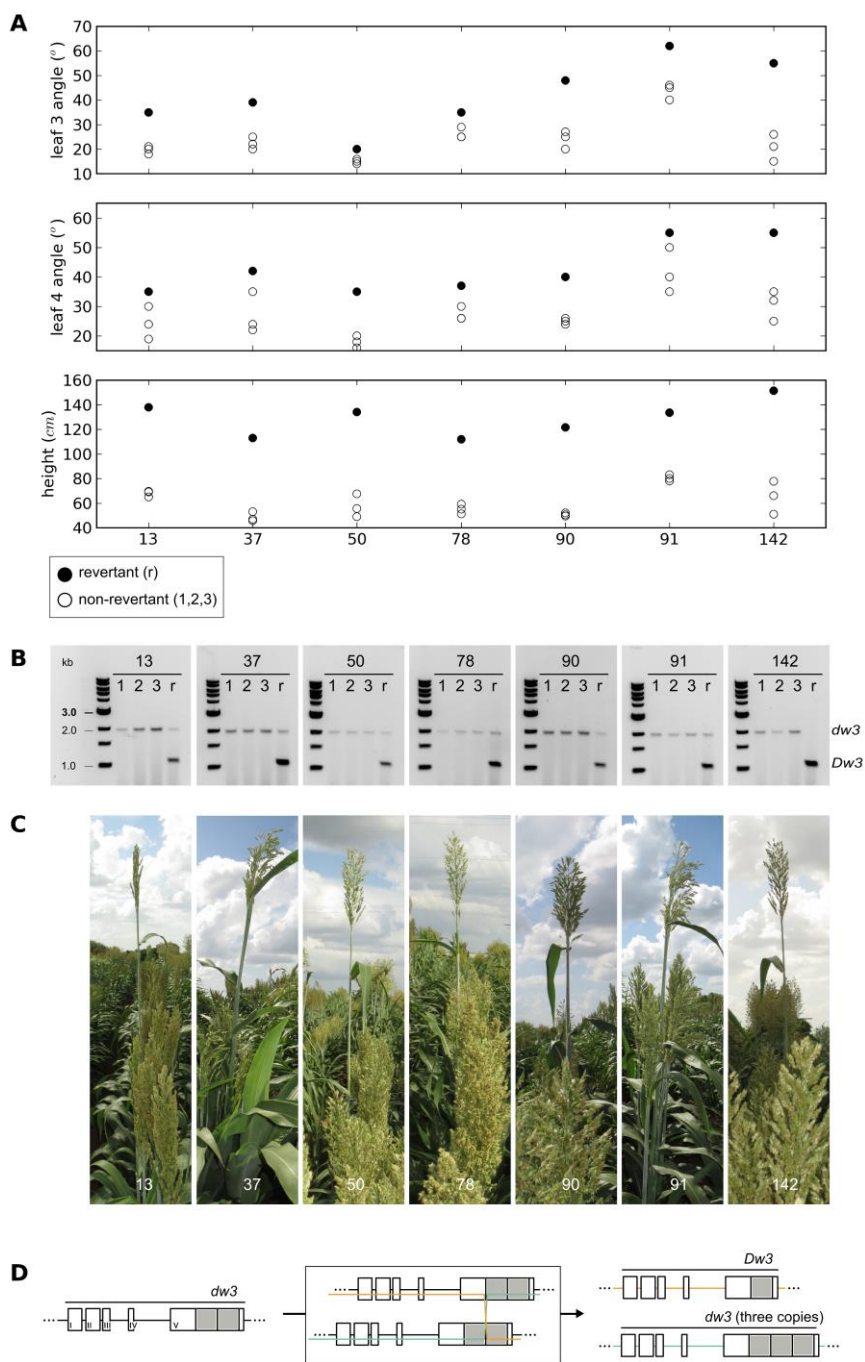


Figure S1 *dw3* regulates leaf inclination angle. **(A)** Phenotypes of *Dw3* revertants (r; filled circles) and non-revertants (1, 2, 3; open circles) of RILs of BTx623 × IS3620C **(B)** Genotypes of revertants and non-revertants of RILs at the *dw3* locus generated using primers designed by FARFAN *et al.* (2012) that flank the 882 bp tandem repeat that makes *dw3* non-functional. Unequal crossing over at *dw3* causes reversion. **(C)** Tall revertants in the row with short non-revertants were identified and genotyped **(A and B)** in the fields in College Station, TX. **(D)** This diagram shows the *dw3* non-functional allele with tandem repeats on exon V as two gray boxes. Unequal crossing over during meiosis results in a revertant functional *Dw3* and a non-functional *dw3* with three copies of the 882 bp sequence.

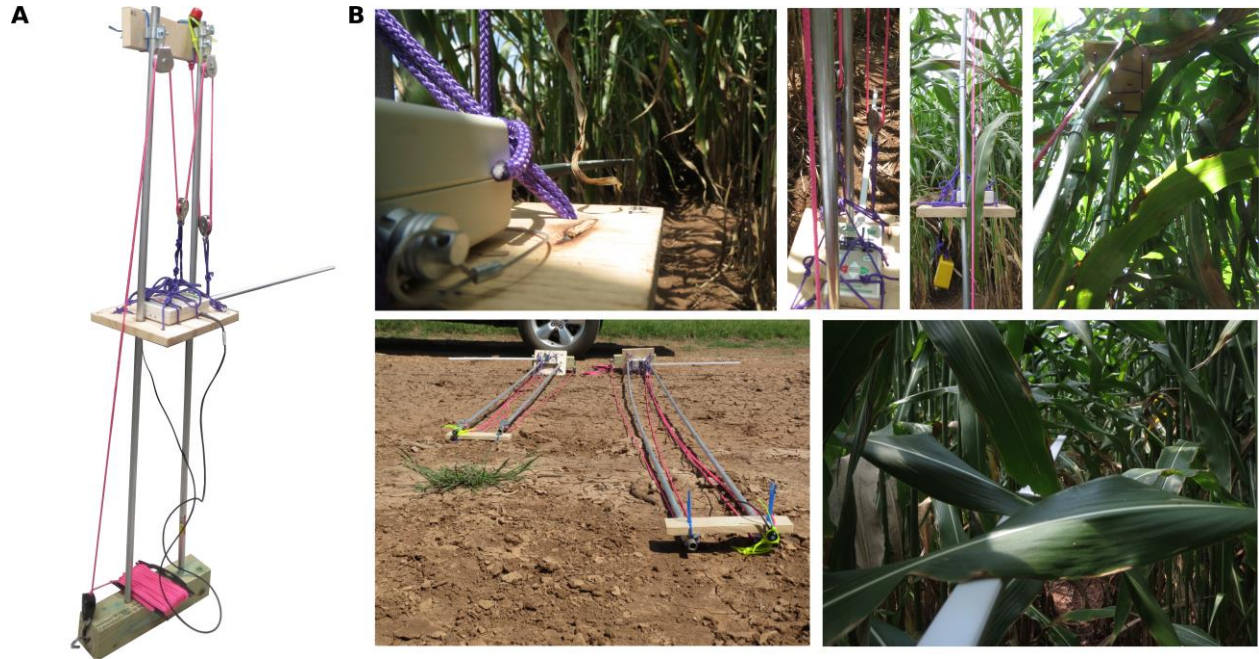


Figure S2 Lift for LP-80 PAR meter. (A) Image of the PAR meter lift used for collection of light measurements within canopies. **(B)** Images of the lift and PAR meter in preparation and in the sorghum canopy. There are views of the wooden platform that the LP-80 sits on and the PAR meter that takes measurements in the canopy. There is also an image of both lifts, where the one on the left has its metal poles extended to 10 ft and the one the right has poles extended to 15 ft.

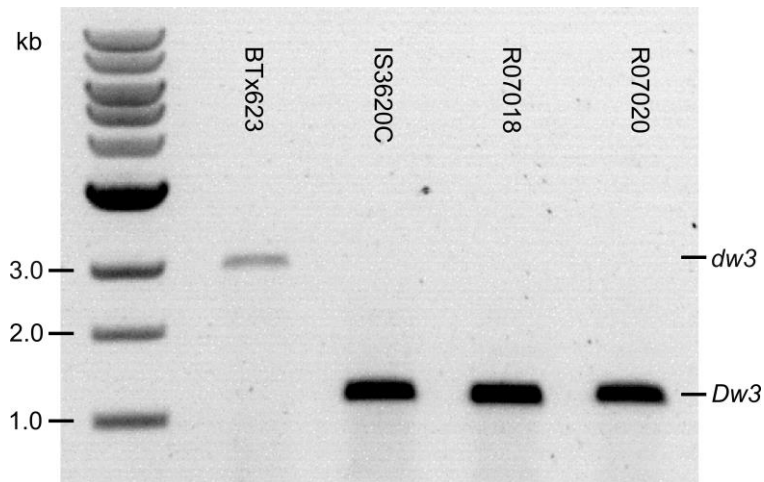


Figure S3 *dwarf-3* genotypes of the bi-parental mapping populations. BTx623, IS3620C, R07018, and R07020 were genotyped at the *dw3* locus generated using primers designed by FARFAN *et al.* (2012) that flank the 882 bp tandem repeat that makes *dw3* non-functional. BTx623 has non-functional *dw3* alleles, while IS3620C, R07018, and R07020 have functional *Dw3* alleles.

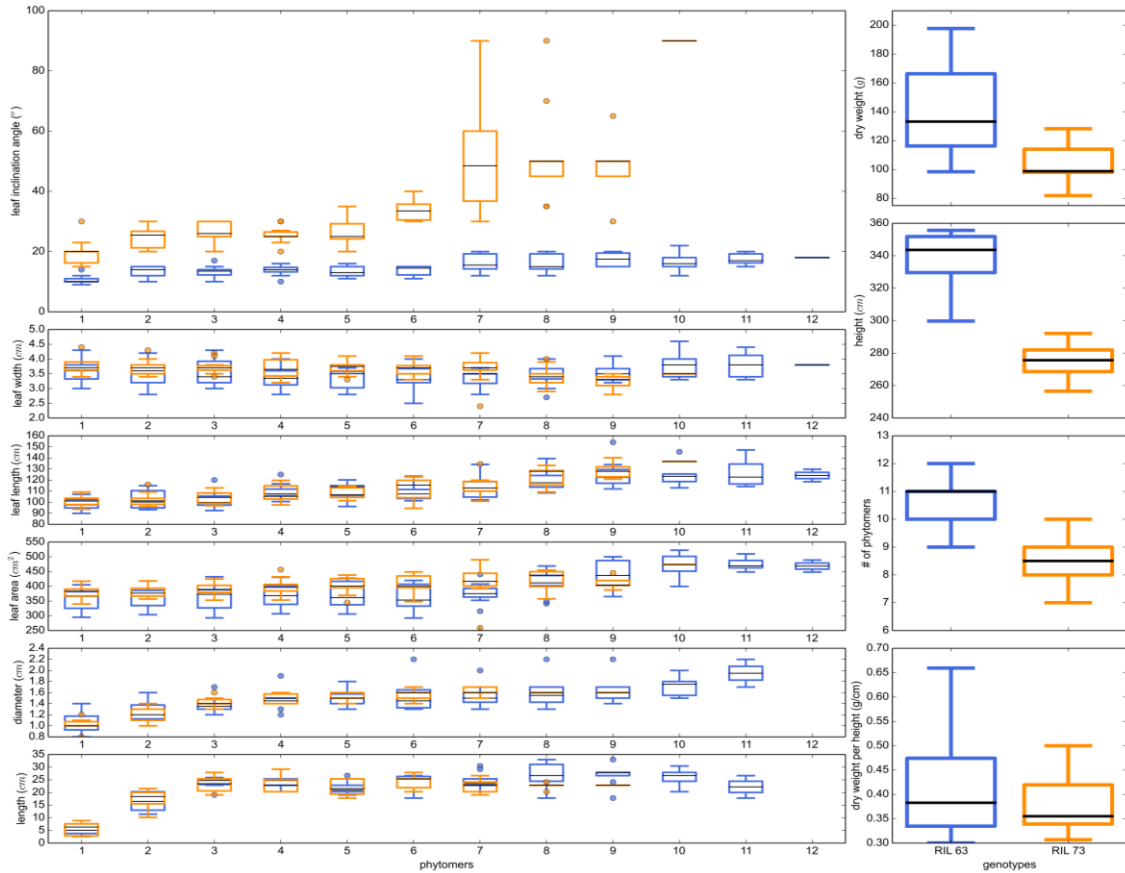


Figure S4 R07018 x R07020 RIL 63 & RIL 73 phenotypes. The boxplots show phenotype data from ten sorghum plants of RIL 63 (blue) and RIL 73 (orange) that were grown in 4-row plots in College Station, TX fields. On the left are measurements by phytomer, where phytomer 1 is at the top of the plant and corresponds to the phytomer with the most recent fully expanded leaf. On the right are measurements of the two genotypes. Leaf chlorophyll (SPAD) was also characterized: RIL 63 with $41.3 \pm 1.5 \text{ nmol/cm}^2$ and RIL 73 with $44.7 \pm 4.0 \text{ nmol/cm}^2$.

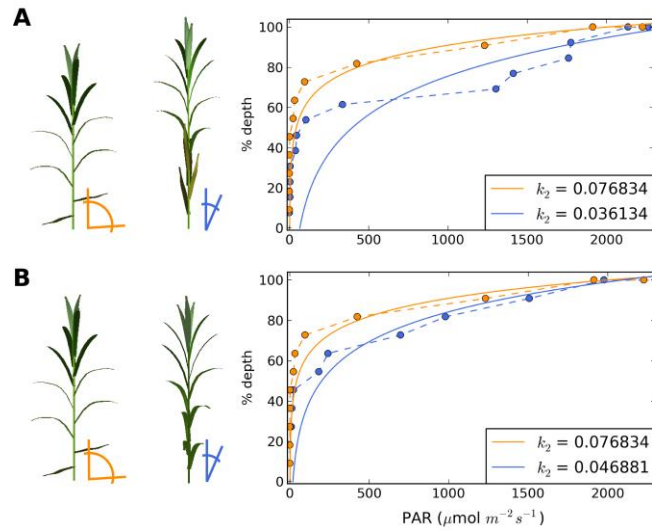


Figure S5 Leaf inclination angle regulates light distribution in canopies. (A) Images of RIL 63 and RIL 73 bioenergy sorghum plants (same as in Figure 2 of the main text). **(B)** Reducing the height of RIL 63 to be the same height as RIL 73 was done by decreasing the number of phytomers. The resulting k of RIL 63 remains smaller than RIL 73 in solar conditions representative of College Station, TX on July 22, 2014 at 15:30. While the qualitative relationship between k values of these plants remains unchanged with respect to height, the change in k that occurs when shortening a plant with RIL 63 angles indicates that height also plays a role in light distribution.

Table S1 Light distribution in canopies of RIL 63 and RIL 73.

Time of acquisition	Height		Scaled depth	
	RIL 73 (large)	RIL 63 (small)	RIL 73 (large)	RIL 63 (small)
July 22 nd at 1400*	0.641993	0.426493	0.065483	0.054250
July 22 nd at 1530*	1.245529	0.392925	0.127043	0.050097
July 23 rd at 1440	0.576724	0.295480	0.060556	0.038412
July 24 th at 1240	0.325723	0.332027	0.034201	0.043828
July 24 th at 1350	0.389599	0.297924	0.040908	0.040220
July 25 th at 1220*	0.374110	0.131663	0.038159	0.017116
July 25 th at 1400*	0.395254	0.210151	0.040316	0.031041

k is calculated with and without scaling depth (height) and scaled depth; the qualitative relationship of k s between RIL 63 (small angles) and RIL 73 (large angles) remain the same. Data was retrieved in July 2014 on the given dates in College Station, TX. “*” denote datasets where RIL 63 was measured by LP-80 #2 and RIL 73 data was measured by LP-80 #1. The LP-80s were switched at other times.

File S2
Additional Supporting Folders and Files

Additional Supporting Folders and Files is available on https://github.com/mulletlab/leafangle_supplement/.

For a detailed work-through of virtual sorghum analysis, custom scripts, .lpy files, and associated parameters are in folder v_sorghum. Data pertaining to field experiments of RIL 63 and RIL 73, and analysis to find *ks* are in folder exp_fields. Specific parameters and additional information for the PCR amplification of *dw3* or *Dw3* are in folder dw3. Genotypes, phenotypes, correlation of phenotypes, genetic linkage maps, heritability calculations and statistics, and multiple QTL mapping penalized LOD scores for each phenotype and the statistics on QTL models presented are in folder h2_and_qtl.

References

- Bartek, M. S., Murray, S.C., Klein, P.E., Mullet, J.E., & Rooney, W.L. , 2012 QTL for biomass yield and composition in energy sorghum (*Sorghum bicolor* L. Moench), pp. in *Science for Biomass Feedstock Production and Utilization SunGrant Conference*. SunGrant Initiative, New Orleans, Louisiana.
- Boudon, F., C. Pradal, T. Cokelaer, P. Prusinkiewicz and C. Godin, 2012 L-py: an L-system simulation framework for modeling plant architecture development based on a dynamic language. *Frontiers in Plant Science* 3: 76.
- Chelle, M., and B. Andrieu, 1998 The nested radiosity model for the distribution of light within plant canopies. *Ecological Modelling* 111: 75-91.
- Chelle, M., Hanan J., & Autret, H. , 2004 Lighting virtual crops: the CARIBU solution for open L-systems, pp. 194 in *4th International Workshop on Functional-Structural Plant Models*, edited by C. Godin, Montpellier, France.
- Farfan, I. D. B., B. R. Bergsma, G. Johal and M. R. Tuinstra, 2012 A stable *dw3* allele in sorghum and a molecular marker to facilitate selection. *Crop Science* 52: 2063-2069.
- Jones, E., Oliphant, T., Peterson, P. et al., 2001 SciPy: Open source scientific tools for Python, pp.
- Long, S. P., X. G. Zhu, S. L. Naidu and D. R. Ort, 2006 Can improvement in photosynthesis increase crop yields? *Plant Cell and Environment* 29: 315-330.
- Monsi, M., and T. Saeki, 2005 On the factor light in plant communities and its importance for matter production. *Annals of Botany* 95: 549-567.
- Monteith, J. L., & Moss, C.J., 1977 Climate and the efficiency of crop production in Britain *Philosophical Transactions of the Royal Society of London, Series B: Biological Sciences* 281: 277-294.
- Nobel, P. S., 2005 *Physicochemical and environmental plant physiology*. Elsevier Academic Press, Amsterdam ; Boston.
- Pradal, C., S. Dufour-Kowalski, F. Boudon, C. Fournier and C. Godin, 2008 OpenAlea: a visual programming and component-based software platform for plant modelling. *Functional Plant Biology* 35: 751-760.
- Prusinkiewicz, P., M. Shirmohammadi and F. Samavati, 2012 L-Systems in geometric modeling. *International Journal of Foundations of Computer Science* 23: 133-146.